FT-IR Difference Spectroscopy of Hemoglobins A and Kempsey: Evidence That a Key Quaternary Interaction Induces Protonation of Asp β99†

Vasilis G. Gregoriou, Vasanthi Jayaraman, Xuehua Hu, and Thomas G. Spiro*

Department of Chemistry, Princeton University, Princeton, New Jersey 08544

Received December 20, 1994®

ABSTRACT: Fourier transform infrared difference spectra are reported for the CO adduct of human hemoglobin versus deoxyHb, in H_2O and D_2O. In addition to the well-known CO stretching and S−H(D) stretching bands, the difference spectra reveal numerous bands in the 1200−1700 cm^{-1} region, a number of which are assigned. Several amide modes are identified via their frequencies and D_2O sensitivities. Bands arising from histidine protonation have also been found via comparison of the difference spectra at different pH(D) values, with the aid of aqueous histidine spectra. Of particular interest is the observation of a negative band at 1697 cm^{-1}, which is assigned to the C=O stretch of carboxylic acid. This carboxylic acid is tentatively identified as the side chain of Asp β99, because it is missing in the difference spectrum of Hb Kempsey, a mutant in which Asp β99 is replaced by Asn. Asp β99 forms a critical contact with Tyr α42 across the $\alpha_1\beta_2$ interface in deoxyHb, which is broken upon ligation. Protonation of Asp β99 in deoxyHb is consistent with UV resonance Raman evidence that Tyr α42 is the acceptor rather than the donor of the quaternary H-bond.

There is continuing interest in the molecular mechanism of cooperative ligand binding by hemoglobin (Hb) (Perutz, 1990). Recent progress in defining intermediate states of the allosteric transition, using chemical modification or kinetic methods, places a premium on techniques for elucidating solution structure (Ackers et al., 1992; Jayaraman et al., 1994). Fourier transform infrared (FT-IR) spectroscopy is becoming an important addition to the arsenal of protein structure techniques (Braiman & Rothschild, 1988; Siebert, 1993). The high precision and dynamic range of interferometry permit the recording of accurate difference spectra with sufficient sensitivity to reveal changes at the single-residue level. In addition, technology is becoming available for time-resolved FT-IR spectroscopy with time resolution sufficient to detect transient intermediates on the millisecond to nanosecond time scales (Braiman et al., 1988; Hartland et al., 1992; Weiderlich & Siebert, 1993).

There have been many studies of the strong CO stretching IR band of HbCO (Alben & Caughey, 1968; Makinen et al., 1979; Potter et al., 1990), and the weak but well-isolated S−H(D) stretching bands of the cysteine residues have also been characterized (Alben & Bare, 1980; Moh et al., 1987). There has been less attention to the crowded region below 1700 cm^{-1}, where protein side chain and backbone vibrations are found. Schliereth and Mantele (1992) have obtained well-resolved difference FT-IR spectra of met- vs deoxyHb (and myoglobin, Mb), using an electrochemical cell, and have suggested a number of assignments. Causgrove and Dyer (1993) have reported detailed difference spectra of MbCO vs deoxyMb in the amide I region, and Miller and Chance (1994) have reported difference spectra between MbCO and its photoproduct in the 1050−1150 cm^{-1} region.

In the present study, we examine HbCO vs deoxyHb difference FT-IR spectra with a view toward elucidating molecular determinants of the R−T quaternary structure change. H/D exchange in D_2O and pH(D) variation are used to assign amide and histidine bands. Of particular interest is the occurrence of a negative difference band at 1697 cm^{-1}, which is assigned to the C=O stretch of a carboxylic acid group in deoxyHb that is unprotonated in HbCO. The absence of this band in Hb Kempsey implicates Asp β99 as the carboxylic acid. In this mutant, asparagine replaces Asp β99, resulting in higher affinity ligand binding and lowered cooperativity. Asp β99 forms a contact with Tyr α42, across the $\alpha_1\beta_2$ subunit interface, which has long been recognized as a critical stabilizing interaction for the T state (Baldwin & Chothia, 1979). This interaction has been assumed to involve H-bond donation from the Tyr OH group to an ionized Asp side chain, but recent evidence from UV resonance Raman spectroscopy indicates that Tyr α42 is an H-bond acceptor in this interaction (Rodgers et al., 1992). The FT-IR carboxylic acid band supports this interpretation.

MATERIALS AND METHODS

Protein Preparation. Adult human hemoglobin (HbA) was prepared from fresh human blood using standard procedures (Antonini & Brunoni, 1971). Red blood cells were exposed to CO, separated by centrifugation in saline solution, and ruptured by dilution in distilled water. After centrifugation to separate the membrane fragments, the HbCO supernatant was stripped of organic phosphates by ion-exchange chromatography. The protein was stored at 77 K; 25 mM potassium phosphate buffer was used for solutions of pH (pD) 5.8 and 7.4, and borate buffer was used for pH (pD) 9.0. NaOH or NaOD was used to adjust the pH (or pD). Samples were dialyzed repeatedly against the appropriate buffer. The protein was left at least 36 h in the pD buffers, in order to allow for exchange of labile protons. DeoxyHb was prepared by photolysis of HbCO with

† This work was supported by NIH Grant GM 25158.

* Author to whom correspondence should be addressed.

® Abstract published in *Advance ACS Abstracts,* April 15, 1995.

0006-2960/95/0434-6876$09.00/0

continuous white light illumination (300 W) at 5 °C under nitrogen. The sample was reconverted to HbCO by exposure to carbon monoxide, so the FT-IR spectra of ligated and deligated species could be recorded with the same sample.

The above procedure was repeated on the Kempsey red blood cells to obtain Hb Kempsey. Hb Kempsey was separated from HbA after passing through a Sephadex G 25 column, by ion-exchange chromatography. A (carboxymethyl)cellulose column (Whatman CM 52) was used in 0.01 M phosphate buffer with a linear ascending pH gradient from 6.9 to 8.0. The collected fraction was concentrated by pressure dialysis; this fraction was then dialyzed versus 25 mM phosphate buffer at pH 6.8 or pD 6.8. The concentration of the Hb samples used for FTIR spectra varied from 2 to 5 mM in heme. All the difference spectra were normalized wit respect to the CO band at 1651 cm^{-1} in order to compare two spectra with different concentrations.

FT-IR Difference Spectroscopy. Spectra were recorded with a Nicolet 800 FT-IR spectrometer operating under dynamic alignment. Its highly stable interferometer permitted reliable measurement of very small intensity differences, $10^{-3}-10^{-5}$ absorbance unit. A high-sensitivity ($D^* = 4 \times 10^{10}$) narrow-band mercury–cadmium–telluride (MCT-A) infrared detector was employed. Double-sided interferograms were collected to ensure proper phase correction. The Mertz phase correction algorithm was utilized with 256 data points taken before and after the zero retardation point. Spectra were collected at 1 cm^{-1} spectral resolution. Data manipulation and analysis were carried out with the Lab Calc software package (Galactic Industries).

CaF_2 windows were used to give unobstructed access to the spectral window above 1000 cm^{-1}, their transparency in the visible region also permitted the aquisition of visible absorption spectra of the loaded FT-IR cell taken before and after infrared measurements to ensure the absence of metHb. Cell spacers were 6 μm (tin, NSG Precision Cells) for H_2O solutions, and 16 μm (Teflon, Spectra Tech) for D_2O solutions. These short path lengths were employed to keep the absorption of the most intense band in the spectrum below 0.9 absorption unit, thereby ensuring linear operation of the IR detector. The actual path length was calculated from the interference fringe pattern of the empty cell.

The temperature of the protein solutions was kept at 14.0 ± 0.1 °C by circulating liquid from a constant-temperature bath (Lauda Model RMS6) around a custom-made IR cell. The thermal gradient between the walls of the IR cell and the solution was monitored with a J-type thermocouple (Omega). This level of control produced difference spectra that exhibit flat line water absorption, since no frequency shifts nor intensity changes of the water absorption bands were observed.

Water vapor absorption lines that result from incomplete purging of the spectrometer present a serious problem in FT-IR difference spectroscopy of proteins, where the signals of interest can be very weak. These lines were subtracted digitally, taking advantage of the high precision of infrared frequency labeling produced by the interference pattern of the HeNe laser reference beam (Griffiths & De Haseth, 1986). The subtraction was carried out interactively with a reference water vapor file of the appropriate resolution and collection parameters that match the parameters of the protein spectrum.

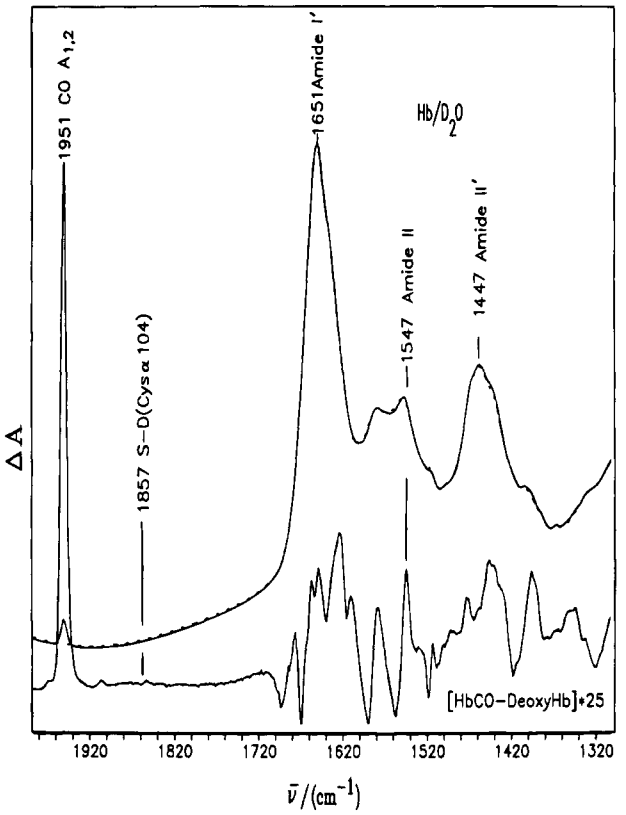

FIGURE 1: Parent FT-IR spectra of HbCO (—) and deoxyHb (– –) (in D_2O at pD 7.4); and their difference multiplied by a factor of 25; 1 cm^{-1} resolution, 1200 scans.

The FT-IR spectra were collected in blocks of 100–400 scans. Block co-addition of scans assures that systematic errors cancel, and that artifacts due to sample deterioration do not accumulate. Consecutive spectra were ratioed and were used to generate the difference spectra (Siebert & Mantele, 1983). The number of co-added spectra ranged from 1000 to 4000 scans, depending on the S/N requirement of the spectral features of interest.

RESULTS AND DISCUSSION

Difference Spectral Quality. Figure 1, obtained in D_2O (pD 7.4) solution, illustrates the spectral quality. The spectra are nearly the same for HbCO and deoxyHb, except for the 1951 cm^{-1} C–O stretching band of HbCO. The strongest bands in the parent spectra arise from the amide vibrations, amide I′ at 1651 cm^{-1} and amide II′ band at 1447 cm^{-1}. A remnant amide II band is also seen at 1547 cm^{-1}, due to unexchanged protons on some of the amide N atoms. The difference spectrum is very weak, and is multiplied by a factor of 25 in the figure.

Figure 2 contains a further scale expansion of the difference spectrum in the 1850–2000 cm^{-1} region, and reveals that the noise level is less than 0.5×10^{-5} absorbance unit. The 1907 cm^{-1} ^{13}CO satellite (1.08% natural abundance) of the 1951 cm^{-1} band is seen very clearly. Also well resolved is the 1968 cm^{-1} band, which arises from a minority substate, designated A_0 (Ormos et al., 1988; Olfield et al., 1991; Makinen et al., 1979; Potter et al., 1990; Ray et al., 1994) of the bound CO, the main band at 1951 cm^{-1} being attributed to overlapping contributions from the majority substates A_1 and A_2. Extensive studies on myoglobin indicate that the higher frequency of the A_0 substate reflects

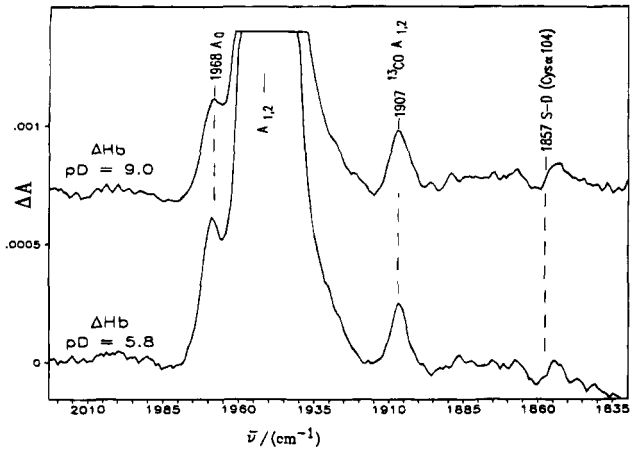

FIGURE 2: Expanded view of the CO and SD stretching region at pD 9.0 and 5.8. The bisignate SD signal is due to a T/R shift in the SD frequency of Cys α104 (Alben & Bare, 1980), while the increase in the A_0 CO intensity at pD 5.8 is attributed to partial protonation of the distal histidine (Morikis, 1989). The ^{13}CO band (1.08% natural abundance) demonstrates the spectra quality.

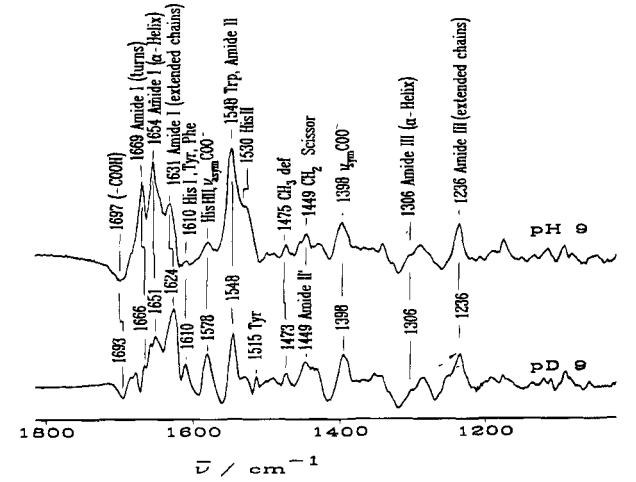

FIGURE 3: Comparison of the FT-IR difference spectrum between HbCO − deoxyHb at pH 9.0 and pD 9.0 in the 1100−1800 cm^{-1} region. Band assignments (see text) are indicated.

an "open" conformation, in which the distal histidine side chain has swung away from the vicinity of the CO (Morikis et al., 1989). This movement can be induced by protonation (Quillin et al., 1992), and the distinct increase in the A_0 intensity in HbCO at pD 5.8 (Figure 2) is consistent with the start of distal histidine protonation. [Its pK_a is ~5.5 (Perutz, 1990).]

Another important spectral feature is the weak bisignate band at 1857 cm^{-1} which results from a shift in the S−D stretching frequency of Cys α104 (Bare et al., 1975; Alben & Bare, 1980), located at the $\alpha_1\beta_1$ subunit interface of Hb. This shift reflects a change in the H-bond status of the residue, and represents an important monitor of quaternary structure. It is encouraging that the spectra permit the observation of a single amino acid residue, having a weak absorption band (ϵ = 60 L mol^{-1} cm^{-1}).

Amide Modes. Figure 3 contains expanded views of difference spectra in the 1200−1700 cm^{-1} region for pH 9 and pD 9 solutions. In the amide I region, the difference intensities are less secure in H_2O because of the large water band at 1640 cm^{-1}. It is nevertheless reassuring that the peaks in H_2O correlate well with the peaks in D_2O, showing

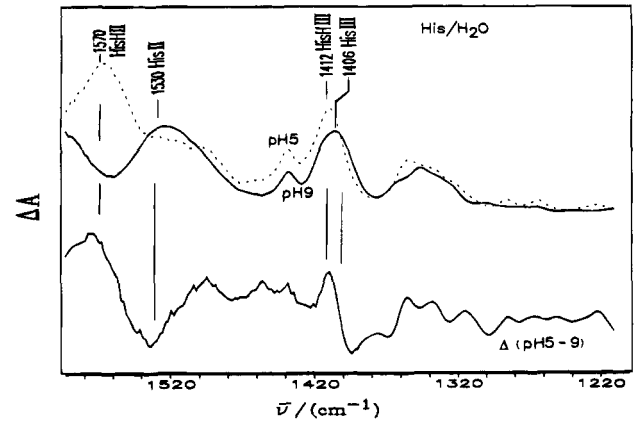

FIGURE 4: FT-IR spectrum of L-histidine (top) at pH 9 (—) and pH 5(- - -). Difference spectrum (bottom).

small downshifts as expected for amide I′ modes. The observed frequencies, 1669, 1654, and 1631 cm^{-1}, are characteristic for peptide bonds in turns, α-helices, and extended chains, respectively (Byler & Susi, 1986; Jacobsen & Wasacz, 1990; Venyaminov et al., 1990a,b; Torii & Tasumi, 1992). There appears to be a slightly greater population of these structures in HbCO than in deoxyHb, or else their IR absorptivities increase. The amide II mode overlaps with a ring mode of tryptophan, but it can be seen to account for most of the 1548 cm^{-1} difference intensity, because of its diminution in D_2O. At the same time, amide II′ intensity appears at 1449 cm^{-1}, as expected. These frequencies are not sensitive to the secondary structure. The amide III frequency is sensitive to secondary structure, but there is little difference intensity in the amide III region (the expected position for α-helices is marked in the figure), except for a band at 1236 cm^{-1}, which might arise from an extended chain structure. Its intensity does not decrease in D_2O, however, so that it must arise from unexchanged peptide bonds if it is indeed amide III (which shifts to much lower frequency upon NH/D exchange).

Other band assignments are suggested in the figure, and some of them are discussed in the following sections.

Histidine. Histidine residues play an important role in the linkage of ligand affinity with pH, the Bohr effect. His β146 is a particularly important residue, accounting for about 40% of the alkaline Bohr effect (Kilmartin, 1977). In deoxyHb, it forms a salt bridge with Asp β94 when it is protonated, but this interaction is lost upon ligation. Consequently, its pK_a drops from 8.1 to 7.0.

The IR spectrum can monitor the histidine protonation state, because some of the imidazole ring modes are sensitive to protonation (Ashikawa & Itoh, 1979). This effect is demonstrated in Figures 4 and 5, which show IR spectra of L-histidine in H_2O and D_2O, at pH(D) 9 and 5, above and below the pK_a for imidazole protonation. In D_2O, the imidazole NH protons exchange, producing alterations in the ring mode composition that change the appearance of the IR spectra. Three prominent bands can be identified which shift upon imidazole protonation, and which produce easily identifiable features in the pH(D) 9 minus 5 difference spectra. We label these His/HisH I, II, and III in H_2O, and I′, II′, and III′ in D_2O. His/HisH I′ are the strongest bands in the D_2O spectra, at 1611 and 1630 cm^{-1}, respectively. We were unable to locate them in H_2O because of strong interference above 1600 cm^{-1} from the water bending band,

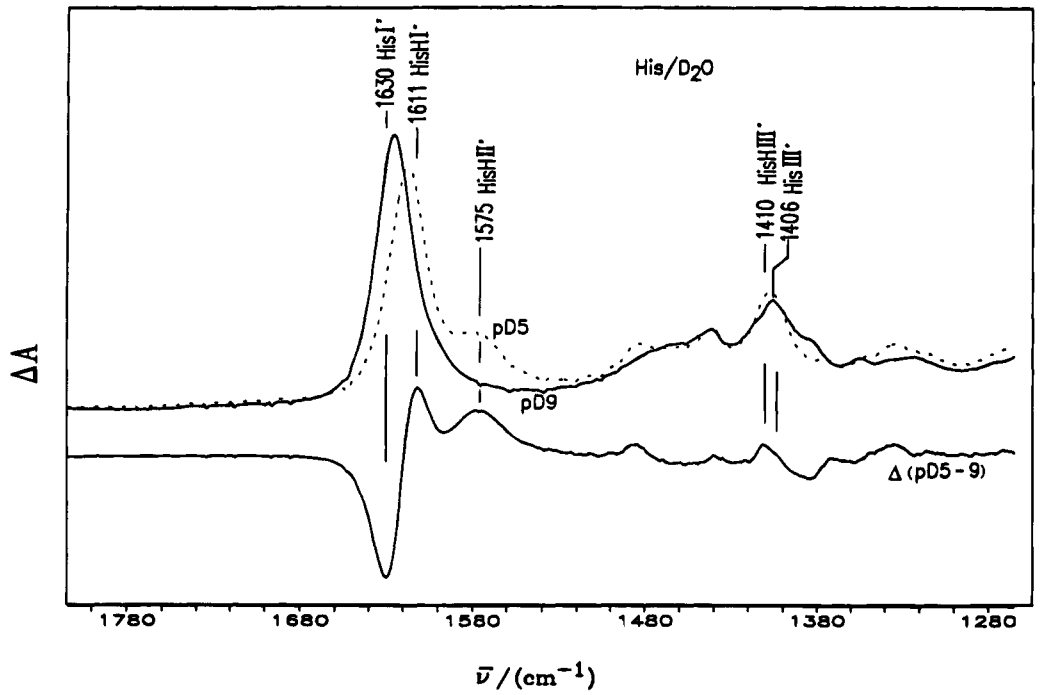

FIGURE 5: FT-IR spectrum of L-histidine (top) at pD 9 (—) and pD 5(- - -). Difference spectrum (bottom).

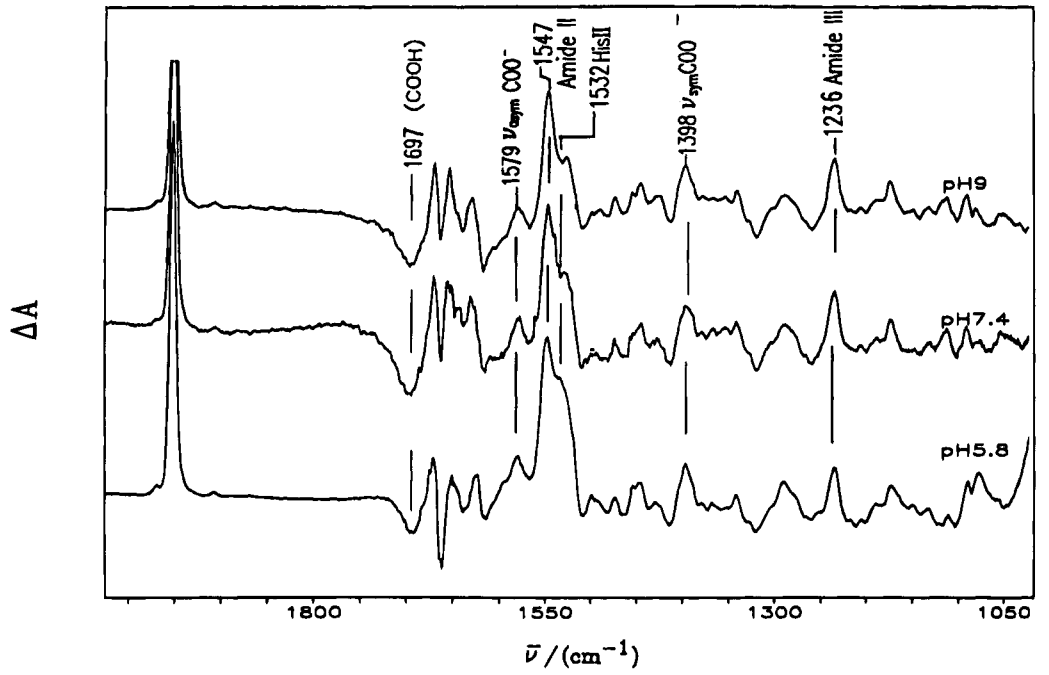

FIGURE 6: Comparison of the FT-IR difference spectrum between HbCO and deoxyHb at pH 5.8, pH 7.4, and pH 9.0.

and also from the N—H bending band of the histidine amino group. HisH II and II' are moderate intensity bands seen at 1570 and 1575 cm^{-1} in the pH 5 spectrum in H_2O and D_2O, respectively, giving rise to a positive difference band. At pH 9, His II appears at 1530 cm^{-1}, producing a negative difference band, but His II' is not seen in the pD 9 spectrum. Finally, His/HisH III and III' are found at 1412/1406 and 1410/1406 cm^{-1}, producing bisignate difference features.

We searched for these features in FTIR difference spectra Hb at different pH values. Figures 6 and 7 show spectra at pH 9, 7.4, and 5.8, in D_2O and H_2O. All the histidine residues should be deprotonated at pH 9, while the release of Bohr protons upon ligation is maximal at pH 7.4 (Kilmartin, 1977). At pH 5.8, the process is reversed, and protons are released upon deligation (acid Bohr effect) (Kilmartin, 1977). Examining the D_2O difference spectra (Figure 6), we see a negative band at 1630 cm^{-1} in the pD 7.4 spectrum, which becomes a small positive band at pD 5.8. At the same time, a positive band at 1610 cm^{-1} becomes stronger at pD 7.4 than 9, but weaker at pD 5.8. This is the expected behavior of the His I' and HisH I' bands if protons are released upon ligation at pD 7.4, but upon deligation at pH 5.8. In H_2O, a band at 1532 cm^{-1} weakens at pH 7.4, but becomes stronger at pH 5.8, as is expected for the His II band. Thus, markers of histidine protonation can be detected in the difference FTIR spectra. However, they occur in crowded regions of the spectrum, and are not easy to monitor. Isotopic labeling of the imidazole ring, especially in a

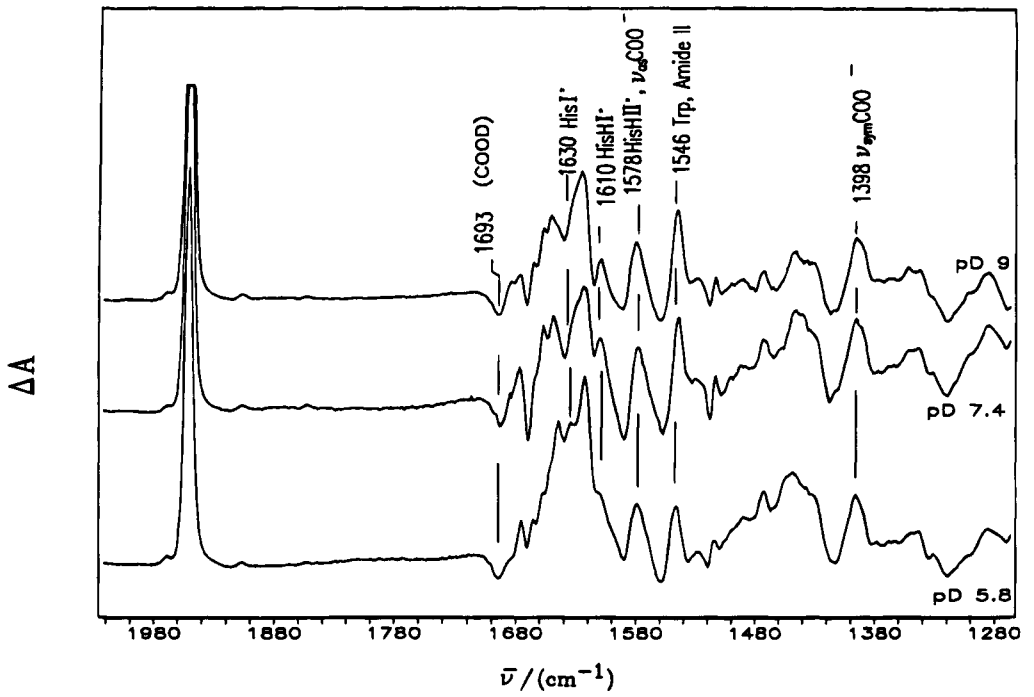

FIGURE 7: Comparison of the FT-IR difference spectrum of HbCO − deoxyHb at pD 5.8, pD 7.4, and pD 9.0. Bands with pD-dependent His contributions are indicated.

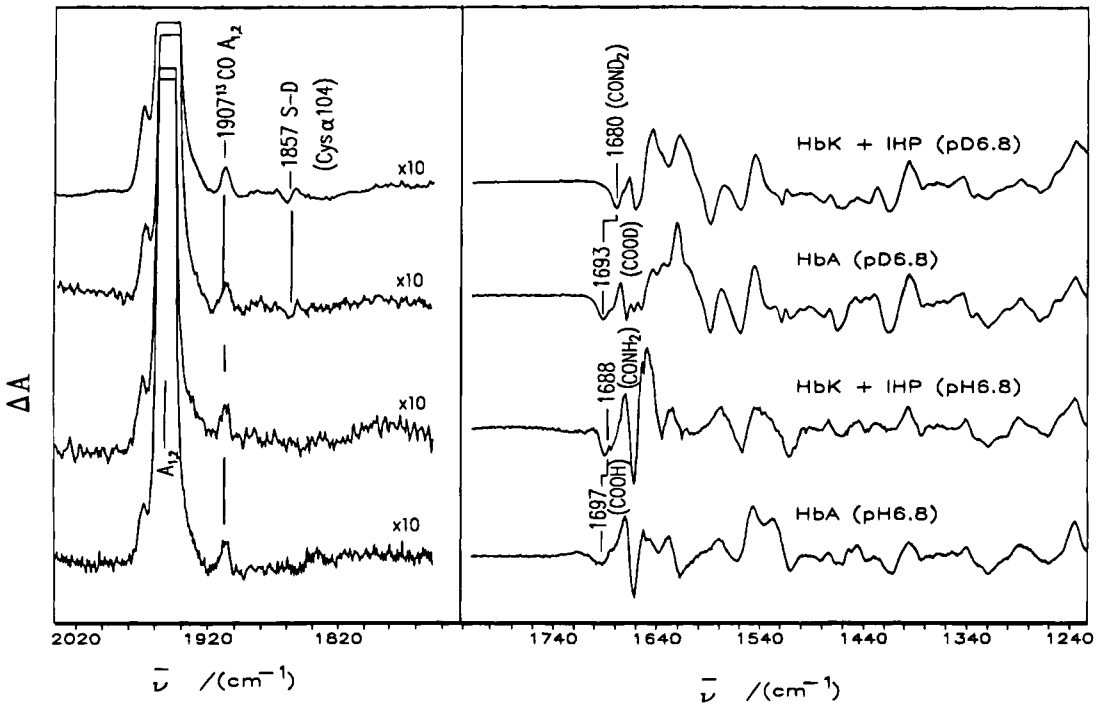

FIGURE 8: Comparison of HbCO − deoxyHb difference FT-IR spectrum for Hb Kempsey and HbA, at pD 6.8 and pH 6.8.

residue-selective manner, would greatly increase the utility of these markers.

Carboxylic Acid Bands; Evidence for Asp β99 Protonation. The difference spectra all show a negative band at 1697 cm^{-1} in H_2O; in D_2O, the band narrows somewhat and shifts to 1693 cm^{-1} (Figure 3). This frequency is in the C=O stretching region. It is at the low end of the scale for carboxylic acids, but is higher than the amide I modes reported for Hb (Byler & Susi, 1986). The C=O frequency is sensitive to the polarity of the environment for both amides and carboxylic acids. A 1697 cm^{-1} frequency suggests strong H-bonding to the C=O group of a carboxylic acid. Since the band is negative, the carboxylic acid must be ionized in HbCO. Positive bands are seen at 1398 and 1578 cm^{-1}, the expected positions for the symmetric and asymmetric stretches, respectively, of carboxylate anions (Gerwert et al., 1990). These bands are in crowded spectral regions, however, and other groups may contribute.

A negative 1697 cm^{-1} band was also seen by Schliereth and Mantele (1993) in the difference FT-IR spectrum of metHb vs deoxyHb. They likewise identified it with carboxylic acid, and suggested a heme propionate assignment. The propionate groups are exposed to solvent, however, and protonation at neutral pH is unlikely (Baldwin

& Chothia, 1979). The spectra in Figures 6 and 7 show that the amplitudes of the 1697 cm^{-1} band, and of the 1398 and 1578 cm^{-1} carboxylate bands, are unaffected by raising the pH to 9. Thus, the carboxylic acid must be inaccessible to solvent in deoxyHb, but accessible in HbCO.

A promising candidate for such a group is the side chain of Asp β99, which forms a quaternary H-bond interaction with Tyr α42 in deoxyHb. This interaction is lost upon ligation, due to the quaternary rearrangement from T to R (Baldwin & Chothia, 1979). The Tyr α42−Asp β99 H-bond is critical to the stability of the T state. Mutants involving Asp β99 have high ligand affinity and low cooperativity (Turner et al., 1992; Bunn et al., 1974; Matsuwaka et al., 1979; Nagai et al., 1975). The H-bond has been assumed to be directed from the Tyr OH group to ionized carboxylate on Asp. However, UVRR difference spectra show upshifted ν_{8a} and ν_{8b} ring modes of Tyr, whereas H-bond donation is known to shift these modes down (Rodgers et al., 1992). This observation suggested that Tyr α42 is instead an H-bond acceptor in deoxyHb, implicating carboxylic acid as the H-bond donor. [Cho et al. (1994) questioned this interpretation because the Tyr excitation profile exhibits a red-shift when IHP is added to metfluoroHb, as it does when Tyr donates an H-bond. However, there are other perturbations that can produce a red-shift, and the excitation profile contains contributions from all six independent Tyr residues in Hb, whereas the deoxyHb minus HbCO difference spectrum is sensitive to the quaternary contacts.] Protonation of Asp β99 is plausible because its side chain is buried in the $\alpha_1\beta_2$ subunit interface, and is not accessible to solvent in the T structure. In the R structure, however, the side chain is partially exposed to solvent (Rodgers et al., 1992). We note that Ho and co-workers (Ho, 1992) assigned the T quaternary marker ^1H NMR reonance at +9.4 ppm to the Tyr α42 OH proton, but while the Tyr α42−Asp β99 H bond is clearly the locus of this resonance, the proton could as well reside on Asp β99 as on Tyr α42.

To test the Asp B99 protonation hypothesis, we determined the CO minus deoxy difference FTIR spectrum of Hb Kempsey, in which Asp β99 is replaced by asparagine (Nagai et al., 1982). The spectrum was compared with that of Hb A in both D_2O and H_2O, under the same pD and pH conditions (Figure 8). Inositol hexaphosphate (IHP) was added to ensure conversion of Hb Kempsey to the T state (Nagai et al., 1982). This conversion was monitored via the S−D stretching difference band at 1857 cm^{-1} (Alben & Bare, 1980). IHP was also added to the Hb A, as a control, but did not affect the difference spectrum.

In H_2O, the 1697 cm^{-1} band is missing in the Hb Kempsey spectrum, and is replaced by a band at 1688 cm^{-1}. The new band is tentatively assigned to the C=O stretch of the Asn β99 side chain, consistent with its downshift to 1680 cm^{-1} in D_2O, as a result of replacement of the primary amide NH_2 protons by deuterons (Dong et al., 1990). This experiment strongly supports the view that Asp β99 is protonated in deoxyHb. This evidence is not conclusive, however, since the Asp→Asn replacement might have an indirect effect on the spectrum, perhaps as a result of a global alteration of the quaternary structure. A definitive assignment of the 1697 cm^{-1} band will require an isotope labeling experiment, which is currently being planned.

The issue of protonation cannot be directly resolved by the X-ray coordinates, and no neutron structure is available for Hb. Nevertheless, it is instructive to examine the Asp β99 environment in the deoxyHb X-ray structure. Figure 9 diagrams the arrangement of neighboring subunits, and shows that either −COOH or COO^- is readily accommodated, as noted previously (Rodgers et al., 1992). Either one accepts H-bonds from Asn α97 and from a water molecule, Wat 4, which is in turn H-bonded to Thr α38. If Asp β99 is protonated, these H-bonds stabilize the developing negative charge on the COOH as it donates an H-bond to Tyr α42. The participation of Wat 4 would explain the low C=O frequency implied by the 1697 cm^{-1} assignment. If Asp β99 is deprotonated, then Tyr α42 forms a third stabilizing H-bond to the COO^-. An energy penalty is nevertheless paid to form the uncompensated negative charge, since Asp β99 is not accessible to solvent in the deoxyHb structure whereas it is partially exposed in the HbCO structure (Rodgers et al., 1992). In this connection, we note that an energy perturbation calculation carried out by Karplus and co-workers (Gao et al., 1989) on a spherical zone surrounding Asp β99, and assuming that it is deprotonated, found three water molecules interacting with the Asp β99 side chain in the deoxyHb structure. The extra two water molecules are

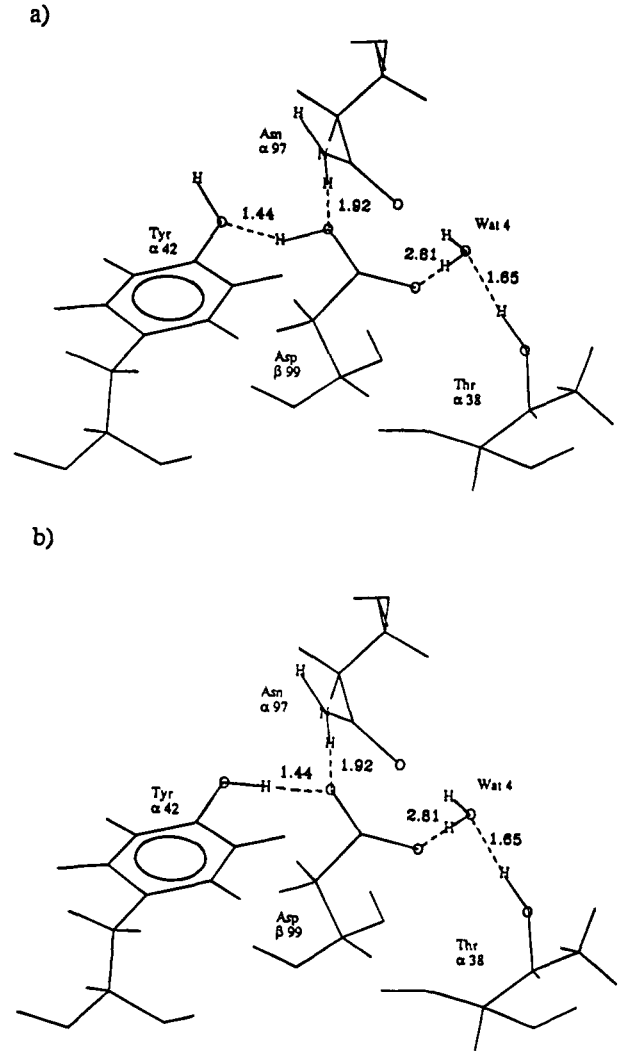

FIGURE 9: H-bonding environment of Asp β99 in deoxyHb from X-ray coordinates (Brookhaven database) Protons are oriented at standard distances and angles. The optimum arrangements for the protonated and unprotonated Asp β99 are shown in (a) and (b), respectively. Estimated H-bond distances are indicated.

not seen in the X-ray structure, however, and were presumably drawn into the interface during the calculation in order to stabilize the anion.

If Asp β99 is protonated in the T state and deprotonated in the R state, then it has major implications for the Bohr effect, the linkage of proton release and ligation. About 2.4 (Perutz, 1990) H^+ are released per Hb tetramer at physiological pH 7.4. Possible sources of these protons have been investigated at length. As was noted above, the two His β146 residues have been estimated to account for 40% of the Bohr protons (Busch et al., 1991; Frier & Perutz, 1977; Kilmartin, 1977). The N-terminal α chain residue, Val α2, loses an ionic interaction (with Cl^- bound to Arg α141) in the R state, resulting in a pK_a reduction which accounts for 25% of the Bohr protons (Kilmartin, 1977). Other histidine residues have been suggested to account for the remainder of the Bohr protons. If, however, each of the Asp β99 residues releases one proton upon ligand binding, then the total proton count is exceeded by at least 45%. The implication would be that there is a counterbalancing uptake of protons accompanying ligation, and that some residues experience pK_a increasses in the T−R transition.

ACKNOWLEDGMENT

We thank Dr. H. F. Bunn of Harvard Medical School for the generous gift of Hb Kempsey, and Dr. Ishita Mukerji for help in its isolation. We also thank Dr. Shankar Subramanian and Dr. George Heibel for helpful discussions; Dr. Heibel kindly prepared Figure 9.

REFERENCES

Ackers, G. K., Doyle, M. L., Myers, D., & Daugherty, M. A. (1992) *Science 255*, 54.
Alben, J. O., & Caughey, W. S. (1968) *Biochemistry 7*, 175.
Alben, J. O., & Bare, G. H. (1980) *J. Biol. Chem. 255*, 3892.
Antonini, E., & Brunori, M. (1971) in *Hemoglobin and Myoglobin and their Reactions with Ligands*, *North*-Holland Publishing Co., Amsterdam.
Ashikawa, I., & Itoh, K. (1979) *Biopolymers 18*, 1859.
Baldwin, J. M., & Chothia, C. J. M. (1979) *J. Mol. Biol. 129*, 175.
Bare, G. H., Alben, J. O., & Bromberg, P. A. (1975) *Biochemistry 14*, 1578.
Braiman, M. S., & Rothschild, K. J. (1988) Annu. *Rev. Biophys. Biophys. Chem. 17*, 541.
Bunn, H. F., Wohl, R. C., Bradley, Cooley, M., & Gibson, Q. H. (1974) *J. Biol. Chem. 249*, 7402.
Busch, M. R., Mace, J. E., Ho, N. T., & Ho, C. (1991) *Biochemistry 30*, 1865.
Byler, D. M., & Susi, H. (1986) *Biopolymers 25*, 469.
Causgrove, T. P., & Dyer, R. B. (1993) *Biochemistry 32*, 11985.
Cho, N., Song, S., & Asher, S. A. (1994) *Biochemistry 33*, 5932.
Dong, A., Huang, P., & Caughey, W. S. (1990) *Biochemsitry 29*, 3303.
Frier, J. A., & Perutz, M. F. (1977) *J. Mol. Biol. 112*, 97.
Gao, J., Kuczera, K., Tidor, B., & Karplus, M. (1989) *Science 244*, 1069.
Gerwert, K., Souvigner, G., & Hess, B. (1990) *Proc. Natl. Acad. Sci. U.S.A. 87*, 9774.
Griffiths, P. R., & De Haseth, J. A. (1986) in *Fourier Transform Infrared Spectroscopy*, John Wiley & Sons, New York.
Hartland, G. B., Xie, W., Dai, H. L., Simon, A., & Anderson, M. J. (1992) *Rev. Sci. Instrum. 63*, 3261.
Ho, C. (1992) *Protein Chem. 43*, 153.
Jacobsen, R. J., & Wasacz, F. M. (1990) *Appl. Spectrosc. 44*, 1478.
Jayaraman, V., Rodgers, K. R., Mukerji, I., Hu, S., & Spiro, T. G. (1995) *Science* (submitted for publication).
Kilmartin, J. V. (1977) *Trends Biochem. Sci. (Pers. Ed.)* 247.
Makinen, M. W., Houtchens, R. A., & Caughey, W. S. (1979) *Proc. Natl. Acad. Sci. U.S.A. 76*, 6042.
Matsukawa, S., Nishibu, M., Nagai, M., Mawatari, K., & Yoneyama, Y. (1979) *J. Biol. Chem. 254*, 2358.
Miller, L. S., & Chance, M. R. (1994) *J. Am. Chem. Soc. 116*, 9662.
Moh, P. P., Fiamingo, F. G., & Alben, J. O. (1987) *Biochemistry 26*, 6243.
Morikis, D., Champion, P. M., Springer, B. A., & Sligar, S. G. (1989) *Biochemsitry 28*, 4791.
Nagai, K., Mar, N. L., Jue, T., & Bunn, H. F. (1982) *Biochemistry 21*, 842.
Nagai, M., Nishibu, M., Sugita, Y., & Yoneyama, Y. (1975) *J. Biol. Chem. 250*, 3169.
Oldfield, E., Guo, K., Auguspurger, J. D., & Dykstra, C. E. (1991) *J. Am. Chem. Soc. 113*, 7537.
Ormos, P., Braunstein, D., Fraunfelder, H., Hong, M. K., Lin, S. L., Sauke, T. D., & Young, R. D. (1988) *Proc. Nat. Acad. Sci. U.S.A. 85*, 8492.
Perutz, M. F. (1990) *Annu. Rev. Physiol. 52*, 1.
Potter, W. T., Hazzard, J. H., Choc, M. G., Tucker, M. P., & Caughey, W. S. (1990) *Biochemistry 29*, 6283.
Quillin, M. L., Brantley, R. E., Jr., Johnson, K. A., Olson, J. S., & Phillips, G. N., Jr. (1992) *Biophys. J. 61*, 466.
Ray, G. B., Li, X.-Y., Ibers, J. A. Sessler, J. L., & Spiro, T. G. (1994) *J. Am. Chem. Soc. 116*, 162.
Rodgers, K. R., Su, C., Subramanian, S., & Spiro, T. G. (1992) *J. Am. Chem. Soc. 114*, 3697.
Schelerth, D. D., & Mantele, W. (1992) *Biochemistry 31*, 7494.
Siebert, F. (1993) in *Biomolecular Spectroscopy, Part A* (Clark, R. J., & Hester, R. E., Eds.) pp 1−54, J. Wiley & Sons, New York.
Siebert, F., & Mantele, W. (1983) *Eur. J. Biochem. 130*, 565.
Torii, H., & Tasumi, M. (1992) *J. Chem. Phys 96*, 3379.
Turner, G. J., Galacteros, F., Doyle, M. L. Hedlund, B., Pettigrew, D. W., Turner, B. W., Smith, F. R., Penn, W. M., Rucknagel, D. L., & Ackers, G. K. (1992) *Proteins: Struct., Funct., Genet. 14*, 333.
Venyaminov, S., Yu., & Kalnin, N. N. (1990a) *Biopolymers 30*, 1243.
Venyaminov, S., Yu., & Kalnin, N. N. (1990b) *Biopolymers 30*, 1259.
Weiderlich, O., & Siebert, F. (1993) *Appl. Spectrosc. 47*, 1394.

BI942926N